Lab on a Chip

Pumpless Microfluidic Devices for Generating Healthy and Diseased Endothelia

Journal:	*Lab on a Chip*
Manuscript ID	LC-ART-05-2019-000446.R1
Article Type:	Paper
Date Submitted by the Author:	17-Jul-2019

Complete List of Authors:	Yang, Yang; University of Maryland at College Park Fathi, Parinaz; University of Illinois at Urbana-Champaign Holland, Glenn; National institute of Standard and technology, Center for Nanoscale Science and Technology Pan, Dipanjan; Washington University, Medicine Wang, Nam Sun; University of Maryland at College Park Esch, Mandy; NIST,

Lab on a Chip

PAPER

Pumpless Microfluidic Devices for Generating Healthy and Diseased Endothelia

Yang Yang,[a,b] Parinaz Fathi,[c] Glenn Holland,[a] Dipanjan Pan,[c] Nam Sun Wang,[b] and Mandy B. Esch [a,†]

Abstract: We have developed a pumpless cell culture chip that can recirculate small amounts of cell culture medium (400 µL) in a unidirectional flow pattern. When operated with the accompanying custom rotating platform, the device produces an average wall shear stress of up to 0.587 Pa ± 0.006 Pa without the use of a pump. It can be used to culture cells that are sensitive to the direction of flow-induced mechanical shear such as human umbilical vein endothelial cells (HUVECs) in a format that allows for large-scale parallel screening of drugs. Using the device we demonstrate that HUVECs produce pro-inflammatory indicators (interleukin 6, interleukin 8) under both unidirectional and bidirectional flow conditions, but that the secretion was significantly lower under unidirectional flow. Our results show that pumpless devices can simulate the endothelium under healthy and activated conditions. The developed devices can be integrated with pumpless tissues-on-chips, allowing for the addition of barrier tissues such as endothelial linings.

Received 00th January 20xx,
Accepted 00th January 20xx

DOI: 10.1039/x0xx00000x

www.rsc.org/

Introduction

Microfluidic tissue culture systems that combine an *in vitro* tissue with an endothelial cell layer simulate nutrient exchange and uptake of drugs more realistically than those that lack such a cell layer. *In vivo*, endothelial cells connect with each other via adherens junctions to form the inner lining of blood vessels.[1] The cell layer presents a barrier to nutrients, waste products, and drugs that must cross it to reach a tissue. Including that barrier in *in vitro* tissues creates more realistic conditions for simulating drug uptake.

Microfluidic tissue-chips are particularly well-suited for culturing the endothelial barrier layer because the medium stream produced in such systems applies mechanical shear to the cells, and mechanical shear is a major modulator of endothelial cell function.[2–4] Both the magnitude and pattern of shear affect the regulation of endothelial proteins, the production of reactive oxygen species (ROS), and the cell layer's barrier function.[2–4] When endothelial cells are cultured within microfluidic tissue-chips, the cell culture medium flow rate and the pattern of shear determine whether endothelial cell layers present an intact or compromised barrier.

Tissue-chips that utilize gravity to drive the needed recirculating fluidic flow are inexpensive, easy to use, and they also provide a range of shear conditions, where the direction of shear can be either unidirectional or bidirectional.[5–10] However, the magnitude of shear and the fluidic flow patterns that can be achieved with current pumpless devices are limited because they depend on the operating ranges of the rocking platforms they are placed on. Rocking platforms are limited with regards to their tilt angle – a typical platform tilts at an angle of about 18° to 20° – and the speed with which the platform can rock back and forth. Both limit the achievable flow conditions. For example, the pulsatile pattern that occurs about 73 times per minute in *in vivo* vessels[11,12] cannot be achieved with devices placed on a rocking platform.

In addition, endothelial cell layers that are exposed to shear that is not unidirectional are activated, presenting a pro-inflammatory phenotype,[13–15] and have been shown to support the development of atherosclerosis,[15,16] and thrombosis *in vivo*.[17] Tissue-chips that provide unidirectional flow and that are capable of producing higher shear and a larger range of shear patterns will be capable of providing more physiologic shear conditions than are currently available with pumpless systems.

Here we have developed a gravity-operated microfluidic chip that produces unidirectional flow and that can be placed at a 90° angle in order to produce up to 0.59 Pa (5.9 dyn/cm^2) of shear. The developed accompanying rotating platform allows us to rotate the chip by 180° at custom time intervals, and if needed, as fast as one rotation per second. That capability creates the opportunity to produce custom flow patterns that cannot be achieved with devices placed on rocking platforms, including pulsatile fluidic flow similar in pattern to that found in mammalian and human blood vessels.[11,12,18]

[a] National Institute of Standards and Technology (NIST), 100 Bureau Drive, Gaithersburg, MD 20899
[b] University of Maryland, Department of Chemical Engineering, College Park, MD
[c] University of Illinois, Department of Biological Engineering, Urbana Champaign, IL
† corresponding author

The developed system can be operated so that it creates periodic waves of unidirectional shear. We show that human umbilical vein endothelial cells (HUVEC) grown in the system, develop the expected healthy monolayers. HUVECs that were grown in control devices where shear periodically reverses direction with a net-shear of zero, developed activated monolayers that were not fully confluent. The developed design allows us to integrate endothelial monolayers that mimic healthy conditions with pumpless microfluidic tissue-chips.

The new design is also capable of supporting endothelial cells with as little as 400 µL of cell culture medium. The capability to recirculate such small amounts of cell culture medium is a design requirement for multi-organ body-on-a-chip systems,[19] and has not been achieved with previous pumpless devices that provide mechanisms for unidirectional flow.[5,20] The presented design and accompanying rotating platform allows us to incorporate healthy endothelial cell layers into gravity-operated multi-organ microphysiologic systems.

Materials and Methods

Microfluidic Device Design

Our goal was to design a microfluidic channel that experiences a stream of cell culture medium with a flow rate similar in magnitude and pattern to what is found in the human microvasculature. We achieved this in a pumpless design that is operated with gravity to drive flow by adjusting the dimensions of the channels, and by placing the devices on a platform that periodically rotates.

We designed the channel, inlet and outlet so that their combined hydraulic resistances allow for a medium flow rate of 1266 µL/min when the device is placed at a 90° angle. We have used this method previously, and briefly describe it here again.[5] The hydraulic resistance for microfluidic channels is given by:

$$R = \frac{12\eta L}{1 - 0.63(\frac{h}{w})} * \frac{1}{(h^3 w)}$$

Eq.1

Here, η is the dynamic viscosity of the cell culture medium, L is the length of the channel, h is the height of the channel, and w is the width of the channel. This equation is valid for channel dimensions that are such that w > h. The overall hydraulic resistance of the fluidic circuit is determined by the sum of the resistances of its in-line elements, like inlet, channel, and outlet:

$$R = (R_{(inlet)} + R_{(channel)} + R_{(outlet)})$$

Eq.2

When the channel is placed at an angle of 90°, the resulting flow rate Q depends on the pressure drop ΔP between inlet and outlet as well as the overall hydraulic resistance of the fluidic circuit:

$$Q = \frac{\Delta P}{R}$$

Eq.3

The pressure drop is calculated using the height difference (h) between inlet and outlet, which is a function of the tilting angle of the device:

$$\Delta P = \rho g h$$

Eq.4

Here, ρ is the density of the cell culture medium in kg/mm^3, and g is the gravity constant. We used these equations to determine the channel height, width, and length that deliver the target maximum wall shear stress of 1 Pa (10 dyn/cm^2).

Our second goal was to recirculate the amount of liquid that flowed through the microfluidic channel, so that the overall amount of liquid present in the system can be kept small. Medium recirculation is an important attribute of tissues-on chips or body-on-a-chip systems when the systems are used to test for the toxicity of drug metabolites.[19] We achieved medium recirculation by adding a second, identical microfluidic channel to the system, and by connecting the two channels via reservoirs that contained passive valve elements.

We also built a custom platform that allowed us to place the device at an angle of 90°, and rotate it periodically by 180° to change the direction of flow. When the device was operated without valves, the cell culture medium went back and forth through the channel, periodically changing its direction. We refer to this type of flow as bidirectional flow. When the device was operated with valves, the cell culture medium went through the two channels in a single direction. This strategy generated periodic, recirculating medium flow without changing direction. We refer to this type of flow as unidirectional flow.

Microfluidic Device Fabrication

The microfluidic devices were fabricated from polydimethyl siloxane (PDMS) using SU-8 masters.‡ The SU-8 masters were made from 500 µm thick dry film sheets we attached to standard, single side polished silicon 100 wafers using a laminator. We used standard contact photolithography processes to create the negative fluidic circuit pattern in SU-8. A thin layer of PDMS (3 mm) was poured onto the silicon masters and cured at 80°C for 60 min. Channel access holes were cut into the PDMS using 0.5 mm biopsy punches. The cast PDMS channels were then placed on large cover glass slips (30 mm x 50 mm). A second, thick layer of PDMS (10 mm) was cast in a petri dish at 80°C for 60 min, and oval reservoir holes were punched with a large diameter biopsy punch (12 mm). The second PDMS layer was visually aligned with the first and placed on top of it (Fig. 1). A third PDMS layer with 2 mm reservoir access holes was also cast and placed on top of the thick reservoir layer (Fig. 1). Sealing is achieved solely through the adhesiveness of PDMS. No other sealant is required. The fully assembled device with cell culture medium is shown in Fig. 2.

Custom Rotating Platform

To gain better control over the angle and time interval the device is held in each position, we built a custom rotating platform. The platform consists of a petri dish holder that can hold up to fourteen petri dishes, a motor, a control unit, and a magnetic proximity sensor. Two small magnets were placed 180° apart from each on the back of the petri dish holder. Once the motor starts rotating the petri dish holder, the proximity sensors will detect one of two magnets rotating by and send a turn-off signal to the motor, stopping the rotation for eight seconds. It was important that the sensor did not take new readings until a second after a new rotation had started. The device is shown in Fig. 3.

Cell Culture

Human umbilical vein endothelial cells (HUVECs, ATCC) were cultured in flasks in a humidified carbon dioxide incubator at 37°C. We used endothelial growth medium (EBM-2) and medium supplements to maintain and grow the cells. For experiments, the cells were detached from the flasks with trypsin. Before seeding the cells into the microfluidic channels, we coated the channels with human fibronectin (5 µg/ml) diluted in phosphate buffered saline for 60 min. Then the cells were loaded into the microfluidic device at a concentration of 150,000 cells/cm^3. To allow for the cells to attach to the channel surfaces, the channels were placed into the incubator for 1 h. After 1 h, we adjusted the amount of cell culture medium in each of the two reservoirs to 200 µL of EBM-2 medium. We started the medium flow by placing the devices into sterile petri dishes, and clamping them onto the rotating platform. The platform placed the dishes at an angle of 90° (Fig 3). It then rotated them by 180° every eight seconds. The medium in the device reservoirs was renewed every day after the initial seeding. The cells were cultured within the fluidic devices for four days.

Cell Staining

To evaluate actin fiber alignment and the presence of vascular endothelial (VE) cadherin, the cells were immunostained with phalloidin conjugated to Alexa 488, and with primary anti VE-cadherin antibodies. The primary antibodies were tagged with secondary antibodies bearing an Alexa 565 color tag. We stained nuclei with DAPI and imaged the cells with an inverted microscope with the appropriate fluorescence filters.

Computational Simulation of Flow Dynamics

A 3D software model of the microfluidic channel was built and imported into COMSOl 5.3. Stationary flow under a series of liquid level differences of the medium inlet and outlet was simulated using COMSOL. Then a polynomial regression curve fitting was applied to the liquid level differences and flow rate. The fluidic flow through the microfluidic channels was simulated in MATLAB R2016b.[‡] Briefly, two partial differential equations (PDEs) for the flow rate in each of the two channel segments were built based on liquid level difference versus flow rate fitting curve, and a third PDE for angular position of the device was built based on the motion of the rotating platform. Then we solved those PDEs via MATLAB PDE solver ode45 with modified absolute tolerance 10^{-13} and relative tolerance 10^{-12}.

Flow Measurements

200 µL of dyed endothelial cell growth basal medium-2 (EBM-2) were added to the empty top reservoir and 200 µL of clear EBM-2 medium was added to the empty bottom reservoir. We video recorded the motion of dyed culture medium in the device at 240 frames per second. Software was used to determine how fast the dyed liquid passed through a 6 mm long channel segment by plotting intensity versus frame at starting point and end point.

To determine the volume flow rate, we added 200 µL EBM-2 with growth factor to the bottom reservoir, then 200 µL of EBM-2 with growth factor to the top reservoir. We then let the medium flow through the device for eight seconds, and then stopped it by removing the culture medium from the top reservoir. The culture medium in the bottom reservoir was collected and weighed. The volume change of culture medium in the bottom reservoir and volume flow rate was calculated. Then the flow rate was adjusted to account for the viscosity difference at room temperature and 37°C.

F-actin angle Measurement

The angle distribution of HUVEC F-actin was analysed via Directionality - a plugin of ImageJ.[‡] The method used here was the Fourier components method. For both HUVECs cultured under unidirectional flow and under bidirectional flow, we obtained three immunofluorescence images per channel and per experiment. Each image captured all cells across the entire width of the channel. From each of the three experiments per condition, we selected one image at random and measured F-actin angles.

Statistical Analysis

The data presented in graphs are the means of at least three separate experiments ± one standard deviation. Comparisons of two mean values with each other was performed using Student's t-tests. A p value of < 0.05 was considered significant and marked with an asterisk.

Results

Device Characterization and Fluidic Flow

The height of the SU-8 pattern on silicon wafers determines the height of the final PDMS channels and with that their hydraulic resistances. To evaluate the SU-8 patter fidelity, we measured six randomly selected positions distributed over a 4" wafer with a surface profilometer. The average height of the channel master was 479 µm ± 2 µm. This was slightly lower than 500 µm, the original thickness of the dry film sheet we used.

Fluidic flow in the microfluidic system is governed by the hydraulic resistances of the channels as well as the differences in liquid levels between the two reservoirs. The height difference between the medium in the reservoirs changes over time as the inlet becomes depleted and the outlet liquid level rises. Every eight seconds, we also switch the position of the reservoirs (Fig. 2). The

resulting flow pattern obtained with mathematical simulations is shown in Fig. 4. The maximum flow rate occurs at the beginning of each cycle, and was calculated to be 1089 µL/min ± 11 µL/min. The maximum wall shear stress at that time is 0.587 Pa ± 0.006 Pa. The average flow rate of three measurements was 845 µL/min ± 23 µL/min. While the average flow rate over 8 seconds obtained from simulations was 914 µL/min ± 9 µL/min. The maximum linear flow velocity at the center streamline was measured to be 53.77 ± 1.68 mm/s.

Unidirectional Design

We operated the microfluidic device so that either unidirectional or bidirectional flow was created in its two channels every eight seconds (Fig. 1). Key to achieving unidirectional flow was to design the two liquid reservoirs as ovals with channel access holes in the upper and lower half of each reservoir (Fig. 2). When the reservoirs are filled with cell culture medium and the device is placed at a 90° angle, fluid will flow from reservoir 1 to reservoir 2 through channel 2 because of gravity (Fig. 2). The flow rate is determined by the hydraulic resistance of channel 2. While medium is flowing through channel 2, channel 1 remains without flow because its access holes are placed at such a position in the reservoirs that at that point in time they are not immersed in medium. In addition, the cell culture medium in channel 1 is prevented from leaving channel 1 because of capillary forces. When the device is rotated by 180°, the flow stops in channel 2, and starts in channel 1 via the same mechanisms. Analysis of time lapse microscopy suggests that devices indeed experienced flow in a single direction. Bidirectional flow is created when the channel access holes are widened so that capillary forces are overcome and fluid is allowed to flow backwards through the channels.

Cell Morphology

We monitored cell morphology and alignment throughout the four-day cell culture period. Microscopy images and fluorescent actin staining show that HUVECs do not align with the direction of flow when they are cultured under flow that periodically changes direction. Cells were not elongated, and actin fibers did not align with the direction of flow. Rather, actin fibers showed frequent accumulations of actin filaments that ended in a single location, producing a star-like pattern (Fig. 5). Under unidirectional flow, HUVECs aligned with the direction of flow as shown by elongated cell bodies, and by actin fibers that were assembled parallel to the direction of flow. The cells grew in complete monolayers with developed adherens junctions visible throughout (Fig. 5).

Analysis of the angle distribution of F-actin showed that F-actin was more likely to align along the direction of flow (i.e. parallel to the channel walls) when cells grew under unidirectional flow, because the overall angle distribution under unidirectional flow was a Gaussian distribution with a standard deviation of 33° (Fig. 6a). Under bidirectional flow, the direction of F-actin fibers was distributed more broadly with a standard deviation of 78° (Fig. 6b). These results are consistent with those obtained in a comparable recent study.[20]

Inflammation

HUVECs cultured under flow that changes direction periodically show signs of inflammation. Immunostaining of VE-cadherin revealed that HUVECs cultured under bidirectional shear developed significant openings in the cell monolayer that exposed the underlying channel surface (Fig. 5). In contrast, when the cells were cultured under unidirectional shear, they built complete monolayers with developed adherens junctions, and without gaps in the cell layer (Fig. 5). In addition, markers that indicate inflammation, such as IL-6, and IL-8 were produced in higher amounts by cells cultured under bidirectional flow when compared with cells cultured under unidirectional flow (Fig. 7). The difference was significant on all three days, except for IL-8 on day four, with a trend of rising values for both conditions over time.

Discussion

Critical Device Parameters for Unidirectional Flow

When operating the device using the rotating platform, i.e. when placing the device at a 90° angle and rotating its position every eight seconds, we did not observe significant back-flow with the unidirectional design. The alignment of the cells with the direction of flow under unidirectional shear and their failure to align with the direction of flow in devices that created bidirectional shear suggests that the two devices generate significantly different conditions that lead to significant differences in the grown endothelial layer. This finding is consistent with those seen in previous studies,[20] and is also supported by the differences in amounts of detected inflammation markers.

The following design elements were critical in achieving unidirectional flow without backflow: a) the channel access holes in both inlet and outlet reservoirs must be small enough to hold cell culture medium via capillary forces inside the channels, b) the channel access holes must be at least 1 mm away from the sidewalls of the reservoirs, and c) the surfaces inside the reservoirs must be smooth and free of any type of grooves. Care must be given to 3D printed designs as well as PDMS designs that were cast on 3D printed molds, because depending on the method and printer chosen, 3D printing can produce grooves that provide capillary forces to liquid in reservoirs. Those forces, if not removed, can allow liquid to flow upwards within a reservoir, enter the channel access holes, and result in backflow.

Additionally, both channel width and height are critical to passively controlling fluidic flow. Here, we calculated a needed channel height of 500 µm, and measured an actual channel height of 479 µm ± 2 µm. This deviation in channel height reduced the flow and wall shear stress to values slightly below those targeted.

When the device was modified to create bidirectional flow, the design elements that are critical to unidirectional flow were reversed so that the channel access holes were large enough to allow for backflow, and the channel access holes were placed close to the reservoir walls. When place on the rotating platform, bidirectional

flow was created in both channel 1 and channel 2 at the same time.

Models of the Endothelium

The pumpless microfluidic device we have developed generates periodic, unidirectional fluidic flow of up to 1089 µL/min ± 11 µL/min, and wall shear stress of up to 0.587 Pa ± 0.006 Pa. The magnitudes of both flow and shear are similar to those observed in mammalian and human blood vessels.[11,12,18] The pattern of flow also approximates that observed in human vessels, although the way we operated the chip, the pattern is only repeated 7.5 times per minute as opposed to a more physiologic repetition rate of about 73 times per minute.[11,12,18] Our devices are capable of producing the physiologic repetition rate, and future use can help with assessing cellular behavior under that flow pattern.

Cells that reside within the device experience periodic changes in shear, similar to that generated by the flow of blood in mammalian and human blood vessels.[11,12,18] When shear forces of this magnitude are applied in a single direction, they support the growth of healthy monolayers of endothelial cells that are aligned with the direction of flow.[2,21–23]

Shear that is unidirectional and that periodically changes its magnitude has been shown to influence the survival and proliferation rates of circulating cancer cells.[24] Fluidic flow can also play a critical role in cell rolling at the blood vessel walls,[25–27] and we envision that our device can be used to investigate the behaviors of circulating cells such as circulating tumor cells or leukocytes.

Cells cultured under bidirectional shear secrete more IL-6, and IL-8 than those cultured under unidirectional shear. Both cytokines are involved in endothelial inflammation,[28,29] indicating that bidirectional shear causes endothelial cells to enter a pro-inflammatory stage. Cells cultured under shear that periodically changes direction also showed more openings in the monolayer, indicating a compromised barrier function. Our results are similar to what others have found when HUVECs are cultured under shear that randomly changes directions.[30,31] Cells cultured in unidirectional mode are comparably healthier, and represent a stage that is likely closer to that of healthy endothelial cells *in vivo*, while those cultured in bidirectional mode resemble cells of an inflamed endothelial lining.

Utility

We show that we can generate healthy and inflamed endothelia by operating a pumpless device. Pumpless designs make it possible to operate many microfluidic systems in parallel in a small space and at low cost. Here we achieved parallel operation using a custom-made rotating platform that can be programmed to rotate in any given time interval (Fig. 1). Although we operated it at 7.5 rotations per minute, we envision using it at higher rotation speeds in the future. Higher rotation speeds will allow us to grow endothelial cells under conditions that mimic physiologic conditions more closely.

The rotating platform can replace the rocking platforms that were previously used for operating pumpless devices.[7,8,20] It is more versatile because it can place microfluidic devices at angles of up to 90°. It can also achieve more complex and faster flow patterns than rocking platforms. Here, we used the rotating platform at 90°, which allowed us to achieve high flow rates and high shear forces.

The design demonstrated here was made from PDMS, because PDMS is a widely used prototyping material. Although we did not use this technique here, PDMS can be coated with materials such as parylene. The coating is suitable to prevent chemical absorption to the device surfaces.[32] The device design is also easy to implement in other materials using other fabrication methods. For example, it can be 3D printed in hydrogels or hard plastics.

Conclusions

We have developed a pumpless microfluidic tissue-chip that when used with a rotating platform generates fluidic flow and shear forces of a magnitude previously measured in human blood vessels. The chip can be operated in unidirectional mode to create flow in one direction, or modified in a way that allows for bidirectional flow that periodically changes direction. The two operating conditions generate endothelial cell monolayers that shows signs of varying degrees of health. Under flow that periodically changes direction, the cell layer exhibits signs associated with inflammation, and under unidirectional flow, the cell layer established a barrier function associated with a healthier status. The device is pumpless and can be operated using a rotation platform. The design can be incorporated into microfluidic tissue-chips so that they can be used to compare nutrient and drug uptake into tissues in the presence of the endothelium. It can also be integrated into pumpless multi-organ microphysiologic devices where cell culture medium must be recirculated among multiple tissue culture chambers. The incorporation of endothelial cells in such devices is an important step toward mimicking drug uptake in the presence of the endothelial barrier or the blood brain barrier.

Conflicts of interest

There are no conflicts of interest to declare.

Acknowledgements

This study was made possible by funds from the Physical Measurement Laboratory (PML) at the National Institute of Standards and Technology (NIST). Nanofabrication for this research project was performed at the NIST Center for Nanoscale Science and Technology (CNST) at NIST under project # N17.0005.03. Yang Yang acknowledges support under the Cooperative Research Agreement between the University of Maryland and the National Institute of Standards and Technology Physical Measurement Laboratory, Award 70NANB14H209, through the University of Maryland. We would like to thank Warren Stewart for drawing and rendering the microfluidic device.

Notes and references

‡ Any mention of commercial products within this work is for information only. It does not imply recommendation or endorsement by NIST.

References

1 W. C. Aird, *Pharmacol. Rep.*, 2008, **60**, 139–43.
2 D. A. Chistiakov, A. N. Orekhov and Y. V. Bobryshev, *Acta Physiol.*, 2017, **219**, 382–408.
3 C. A. Reinhart-King, K. Fujiwara and B. C. Berk, in *Methods in enzymology*, 2008, vol. 443, pp. 25–44.
4 K.-S. Heo, K. Fujiwara and J. Abe, *Mol. Cells*, 2014, **37**, 435–40.
5 M. B. Esch, H. Ueno, D. R. Applegate and M. L. Shuler, *Lab Chip*, 2016, **16**, 2719–2729.
6 M. B. Esch, J. M. Prot, Y. I. Wang, P. Miller, J. R. Llamas-Vidales, B. A. Naughton, D. R. Applegate and M. L. Shuler, *Lab Chip*, 2015, **15**, 2269–2277.
7 C. Oleaga, C. Bernabini, A. S. T. Smith, B. Srinivasan, M. Jackson, W. McLamb, V. Platt, R. Bridges, Y. Cai, N. Santhanam, B. Berry, S. Najjar, N. Akanda, X. Guo, C. Martin, G. Ekman, M. B. Esch, J. Langer, G. Ouedraogo, J. Cotovio, L. Breton, M. L. Shuler and J. J. Hickman, *Sci. Rep.*, 2016, **6**, 20030.
8 P. G. Miller and M. L. Shuler, *Biotechnol. Bioeng.*, 2016, **113**, 2213–2227.
9 S. Alimperti, T. Mirabella, V. Bajaj, W. Polacheck, D. M. Pirone, J. Duffield, J. Eyckmans, R. K. Assoian and C. S. Chen, *Proc. Natl. Acad. Sci.*, 2017, **114**, 8758–8763.
10 V. Van Duinen, A. Van Den Heuvel, S. J. Trietsch, H. L. Lanz, J. M. Van Gils, A. J. Van Zonneveld, P. Vulto and T. Hankemeier, *Sci. Rep.*, , DOI:10.1038/s41598-017-14716-y.
11 C. A. Taylor, C. P. Cheng, L. A. Espinosa, B. T. Tang, D. Parker and R. J. Herfkens, *Ann. Biomed. Eng.*, 2002, **30**, 402–8.
12 S. Oyre, E. M. Pedersen, S. Ringgaard, P. Boesiger and W. P. Paaske, *Eur. J. Vasc. Endovasc. Surg.*, 1997, **13**, 263–271.
13 J. Ando and K. Yamamoto, *Circ. J.*, 2009, **73**, 1983–92.
14 O. Traub and B. C. Berk, *Arterioscler. Thromb. Vasc. Biol.*, 1998, **18**, 677–85.
15 N.-T. Le, K.-S. Heo, Y. Takei, H. Lee, C.-H. Woo, E. Chang, C. McClain, C. Hurley, X. Wang, F. Li, H. Xu, C. Morrell, M. A. Sullivan, M. S. Cohen, I. M. Serafimova, J. Taunton, K. Fujiwara and J. Abe, *Circulation*, 2013, **127**, 486–499.
16 K.-S. Heo, K. Fujiwara and J.-I. Abe, *Mol. Cells*, 2014, **37**, 435–440.
17 K. C. Koskinas, Y. S. Chatzizisis, A. P. Antoniadis and G. D. Giannoglou, *J. Am. Coll. Cardiol.*, 2012, **59**, 1337–1349.
18 M. Intaglietta, D. Richardson and W. Tompkins, *Am. J. Physiol. Content*, 1971, **221**, 922–928.
19 M. B. Esch, A. S. T. Smith, J. M. Prot, C. Oleaga, J. J. Hickman and M. L. Shuler, *Adv. Drug Deliv. Rev.*, 2014, 69–70, 158–169.
20 Y. I. Wang and M. L. Shuler, *Lab Chip*, 2018, **18**, 2563–2574.
21 J. Ando and A. Kamiya, *Front. Med. Biol. Eng.*, 1993, **5**, 245–64.
22 C. M. F. Potter, M. H. Lundberg, L. S. Harrington, C. M. Warboys, T. D. Warner, R. E. Berson, A. V Moshkov, J. Gorelik, P. D. Weinberg and J. A. Mitchell, *Arterioscler. Thromb. Vasc. Biol.*, 2011, **31**, 384–391.
23 B. J. Ballermann, A. Dardik, E. Eng and A. Liu, *Kidney Int. Suppl.*, 1998, **67**, S100-8.
24 R. Fan, T. Emery, Y. Zhang, Y. Xia, J. Sun and J. Wan, *Sci. Rep.*, 2016, **6**, 27073.
25 Q. Huang, X. Hu, W. He, Y. Zhao, S. Hao, Q. Wu, S. Li, S. Zhang and M. Shi, *Am. J. Cancer Res.*, 2018, **8**, 763–777.
26 J. J. Jung, K. A. Grayson, M. R. King and K. A. Lamkin-Kennard, *Microvasc. Res.*, 2018, **118**, 144–154.
27 P. Sundd, M. K. Pospieszalska, L. S.-L. Cheung, K. Konstantopoulos and K. Ley, *Biorheology*, 2011, **48**, 1–35.
28 A. Dubiński and Z. Zdrojewicz, *Pol. Merkur. Lekarski*, 2007, **22**, 291–4.
29 A. Harada, N. Sekido, T. Akahoshi, T. Wada, N. Mukaida and K. Matsushima, *J. Leukoc. Biol.*, 1994, **56**, 559–564.
30 M. Dabagh, P. Jalali, P. J. Butler, A. Randles and J. M. Tarbell, *J. R. Soc. Interface*, , DOI:10.1098/rsif.2017.0185.
31 S. Chien, *Ann. Biomed. Eng.*, 2008, **36**, 554–562.
32 Y. S. Shin, K. Cho, S. H. Lim, S. Chung, S.-J. Park, C. Chung, D.-C. Han and J. K. Chang, *J. Micromechanics Microengineering*, 2003, **13**, 768–774.

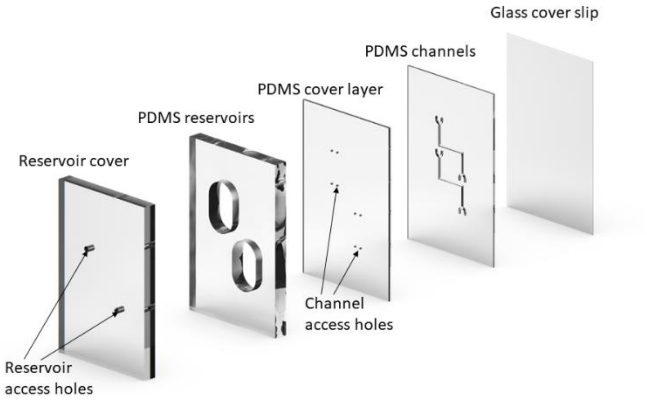

Figure 1: Layers of the microfluidic device. The device consists of a thin glass layer and several PDMS layers. A key feature of the design are the channel access holes through which cell culture medium can leave the upper reservoirs to flow into the lower reservoir. To create unidirectional flow it is important that the channel access holes are placed at the top and bottom region of the reservoir, and at least 1 mm away from the reservoir walls.

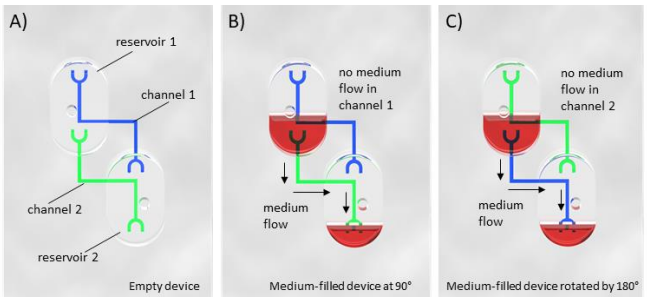

Figure 2: Microfluidic device. There are two separate fluidic channels that together make up the circuit (A). Each channel contains HUVEC. When cell culture medium is added to the reservoirs, it first fills both channels. When the device is placed at a 90° angle, medium flows through channel 2, but not through channel 1 (B). At the beginning of that cycle, reservoir 1 is full and reservoir 2 is still empty. After 8 s of fluidic flow, reservoir 1 is nearly empty, and reservoir 2 is filled. Then the device is turned by 180°, medium flows through channel 1, but not channel 2 (C).

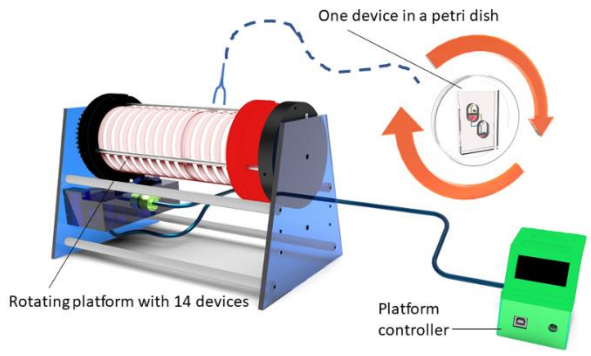

Figure 3: Rotating platform. Microfluidic devices are placed in petri dishes and placed vertically into the platform. The platform holds up to 14 petri dishes. For this study we rotated the petri dishes by 180° every eight-seconds. Details of the fluidic device are shown in Fig. 1.

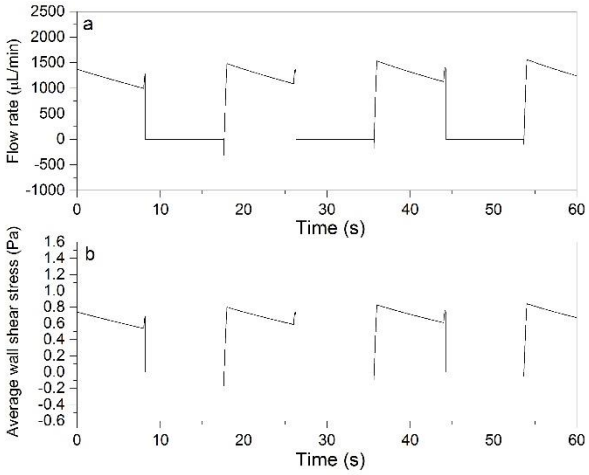

Figure 4: Calculated flow rates and shear inside the microfluidic channels during device operation.

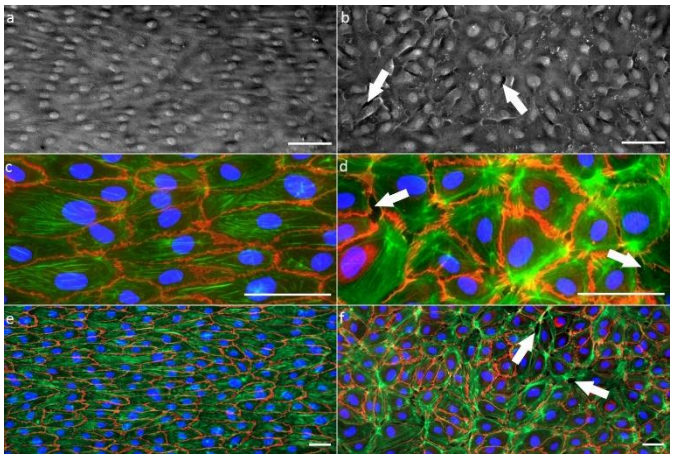

Figure 5: Optical microscopy images and fluorescence microscopy images of HUVECs cultured within the microfluidic devices under unidirectional flow (a, c, e), and under bidirectional flow (b, d, f). The white arrows point at locations where the barrier function of the cell layer is not fully developed. Green: phalloidin-Alexa 488 stained actin, red: immunostained VE-cadherin, blue: DAPI stained nuclei. All scale bars represent 50 µm.

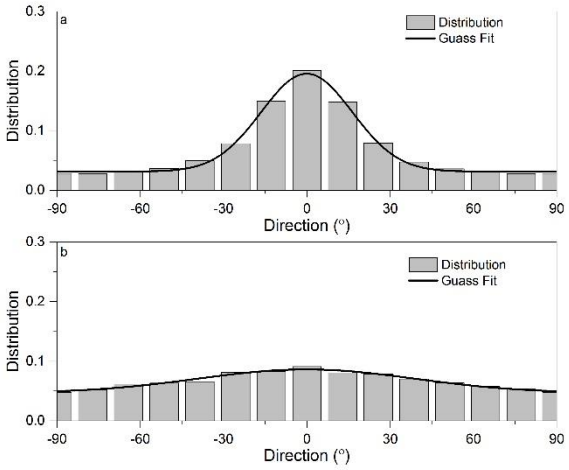

Figure 6: Distribution of actin fiber angles in HUVECs cultured under unidirectional (a) and bidirectional flow (b). Data represent data collected from three separate experiments per condition.

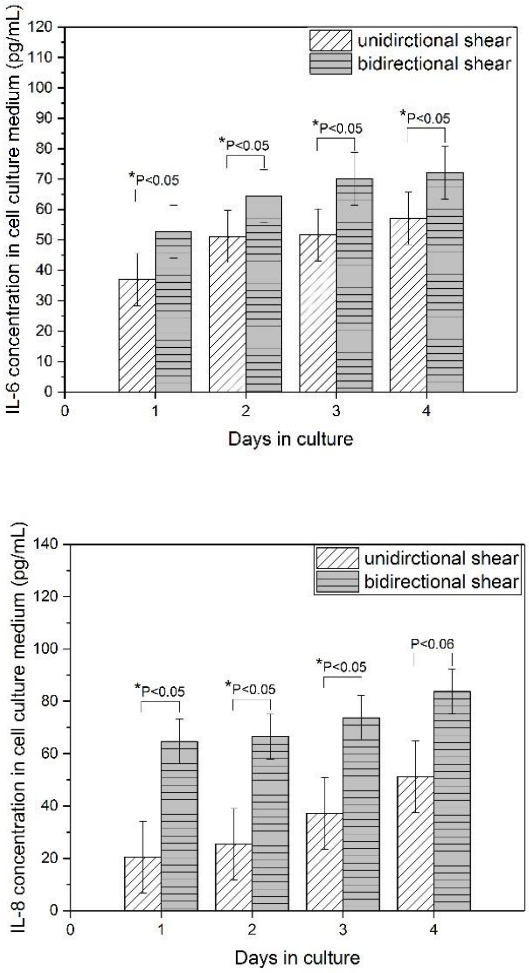

Figure 7: Amounts of IL-6 (A) and IL-8 (B) in the medium collected from human umbilical vein endothelial cells cultured under waves of unidirectional or bidirectional shear. Data represent the mean of at least three experiments, and error bars represent standard deviations.